

## Supporting Information

### Experimental and Theoretical Study for *Dimer-of-Dimers*-type Tetrarhodium(II) Complexes Bridged by 1,4-Benzenedicarboxylate Linkers

Yusuke Kataoka,<sup>a,\*</sup> Kazuki Arakawa,<sup>a</sup> Hikaru Ueda,<sup>a</sup> Natsumi Yano,<sup>a</sup> Tatsuya Kawamoto,<sup>b</sup> and Makoto Handa<sup>a,\*</sup>

<sup>a</sup>Department of Chemistry, Interdisciplinary Graduate School of Science and Engineering, Shimane University, 1060, Nishikawatsu, Matsue, 690-8504, Japan.

<sup>b</sup>Department of Chemistry, Faculty of Science, Kanagawa University, 2946, Tsuchiya, Hiratsuka, Kanagawa, 259-1293, Japan.

---

#### Index

Figure S1. Observed (top) and simulated (1+: middle, 2+: bottom) ESI-MS of **[1]**.

Figure S2. Observed (top) and simulated (1+: middle, 2+: bottom) ESI-MS of **[2]**.

Figure S3. Crystal structure of **[1(THF)<sub>4</sub>]** refined with disorder.

Figure S4. Relative total energies of **[1(THF)<sub>4</sub>]** and **[2(THF)<sub>4</sub>]** calculated by DFT-D calculations.

Figure S5. MOs of **[1(THF)<sub>4</sub>]**.

Figure S6. MOs of **[2(THF)<sub>4</sub>]**.

Figure S7. LUMOs ( $\beta$  orbitals) of **[1(THF)<sub>4</sub>]<sup>+</sup>** and **[2(THF)<sub>4</sub>]<sup>+</sup>**

Figure S8. The plots of orbital energies of HOMOs vs. one-electron oxidization potentials of **[1]**, **[2]**, and **[Rh<sub>2</sub>(piv)<sub>4</sub>]**.

Table S1. Selected structural parameters (bond lengths: Å, angles: °) of crystal structure of **[1(THF)<sub>4</sub>]**.

Table S2. Selected structural parameters (bond lengths: Å, angles: °) of crystal structure of **[2(THF)<sub>4</sub>]**.

Table S3. The averaged bond lengths of optimized geometries of **[1(THF)<sub>4</sub>]** and **[2(THF)<sub>4</sub>]**.

Table S4. TDDFT results (excitation energies, oscillator strengths, and assignments) of **[1(THF)<sub>4</sub>]**.

Table S5. TDDFT results (excitation energies, oscillator strengths, and assignments) of **[2(THF)<sub>4</sub>]**.

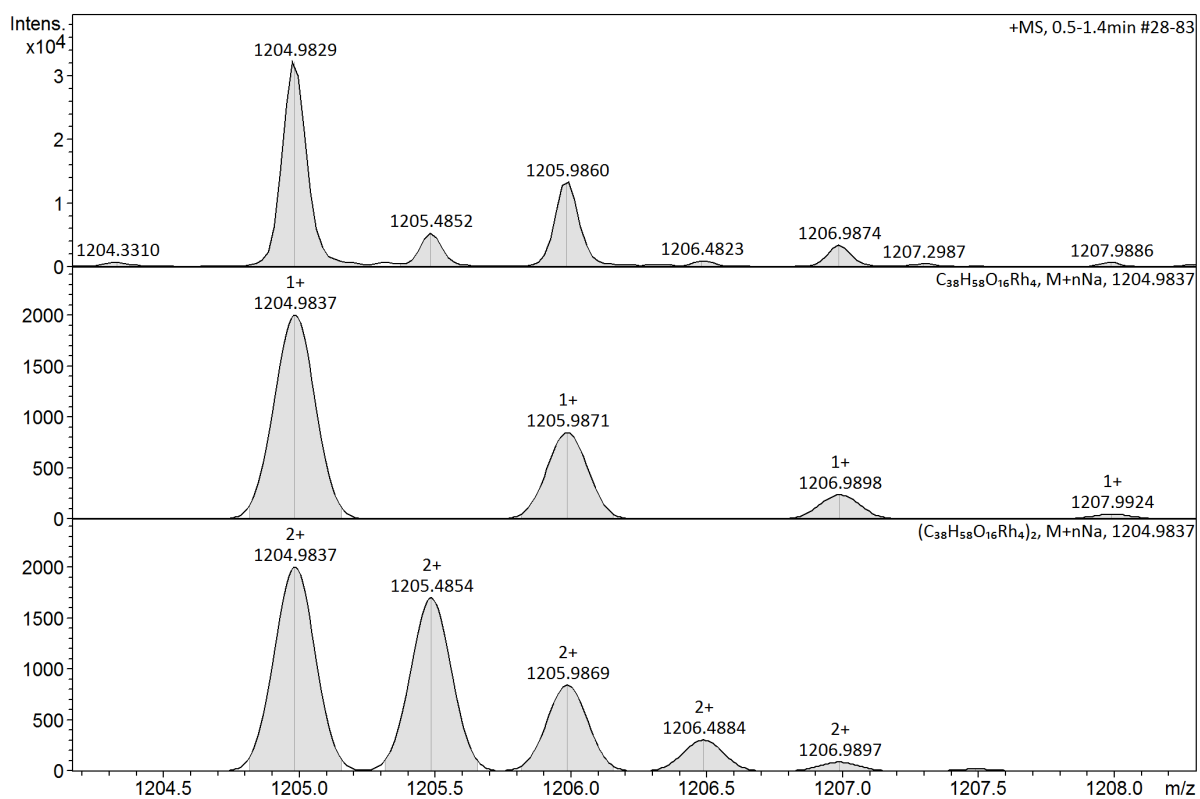


Figure S1. Observed (top) and simulated (1+: middle, 2+: bottom) ESI-MS of [1].

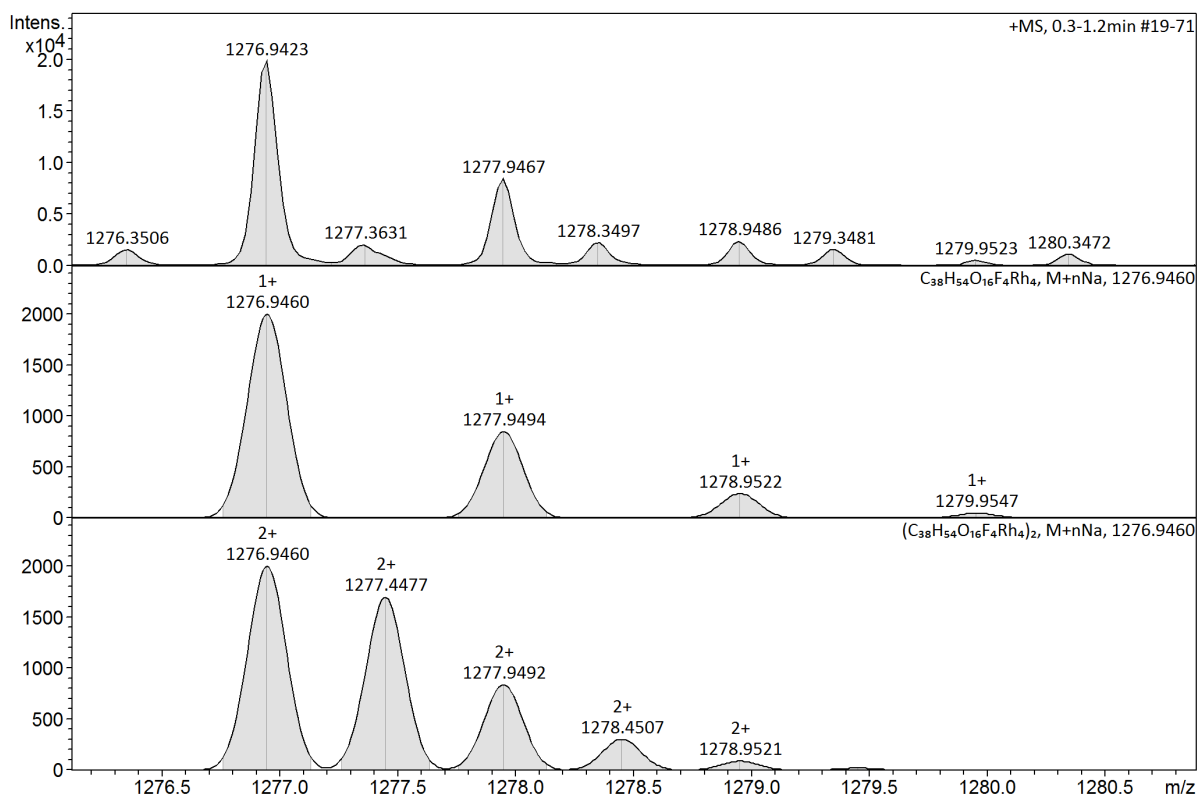


Figure S2. Observed (top) and simulated (1+: middle, 2+: bottom) ESI-MS of [2].

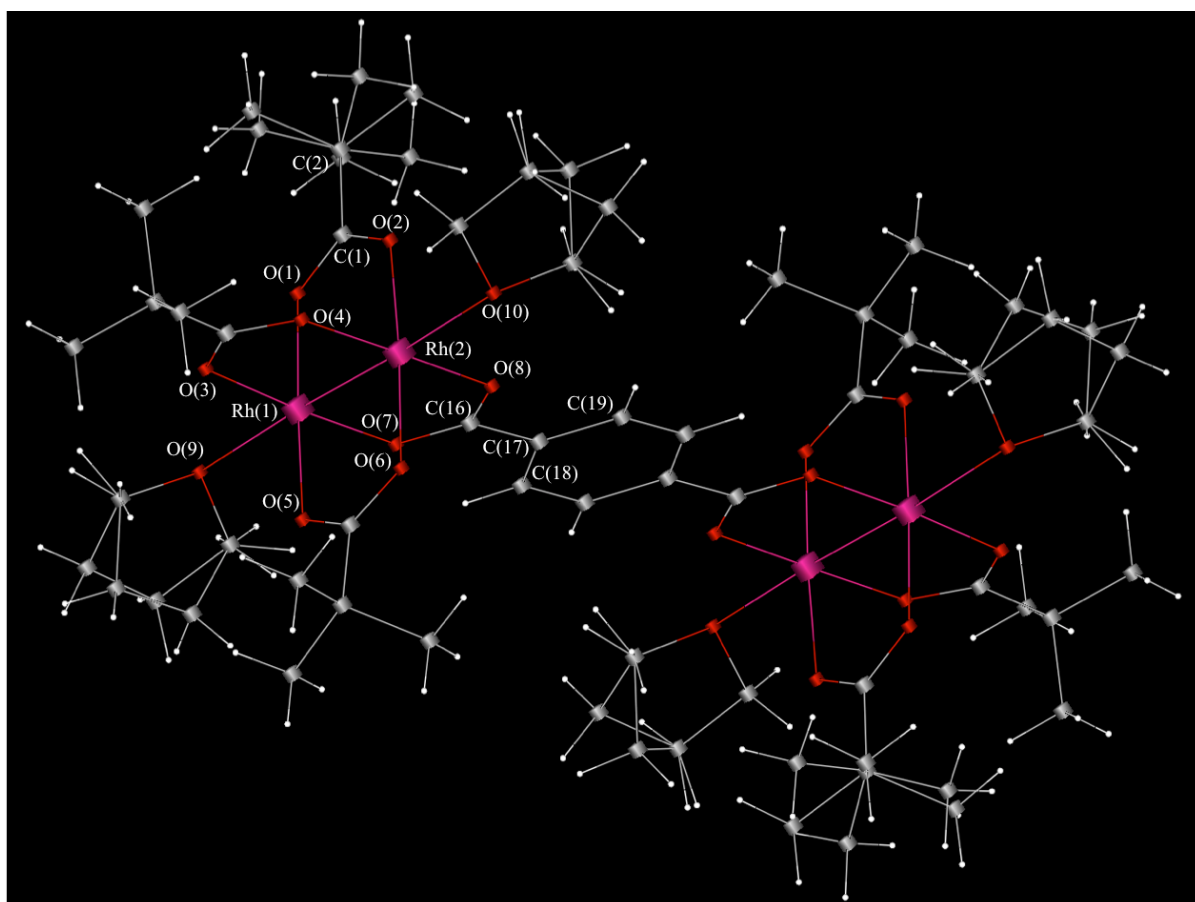


Figure S3. Crystal structure of [1(THF)<sub>4</sub>] refined with disorder.

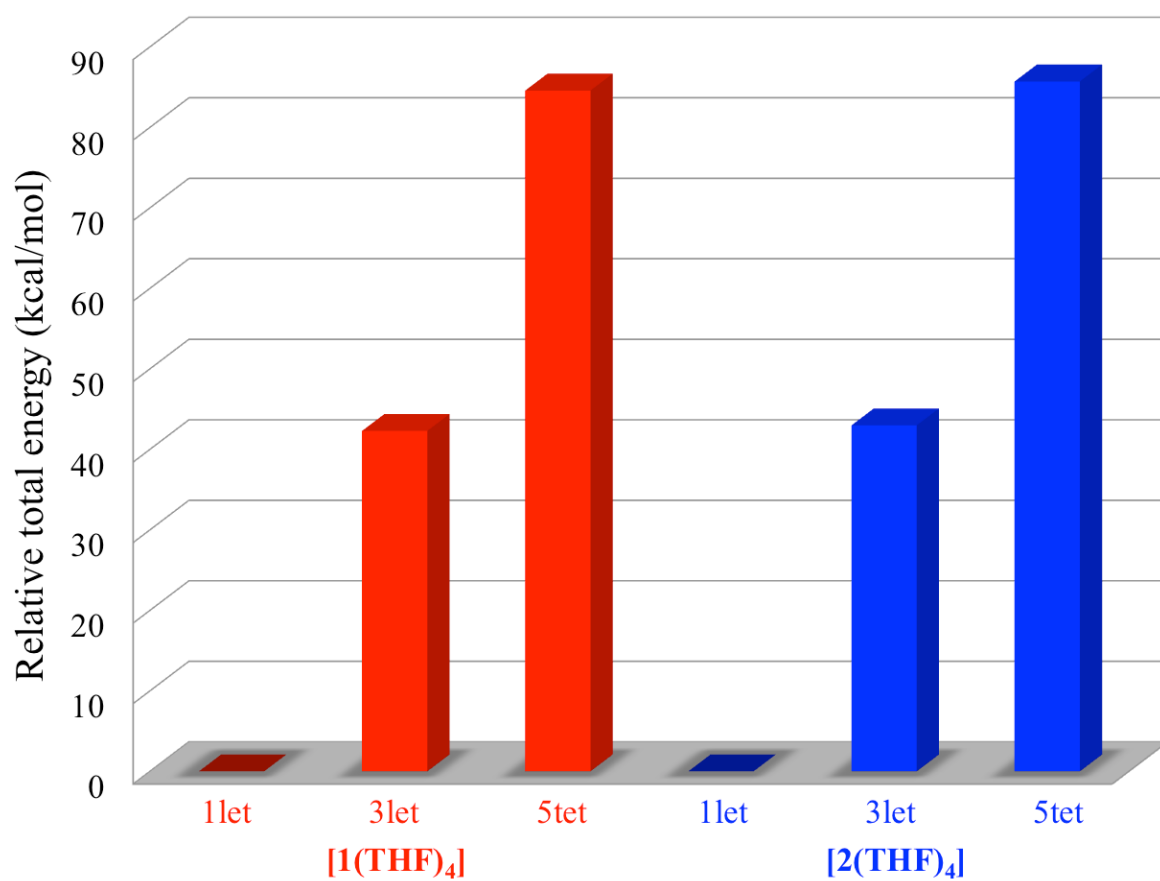


Figure S4. Relative total energies of [1(THF)<sub>4</sub>] and [2(THF)<sub>4</sub>] calculated by DFT-D calculations.

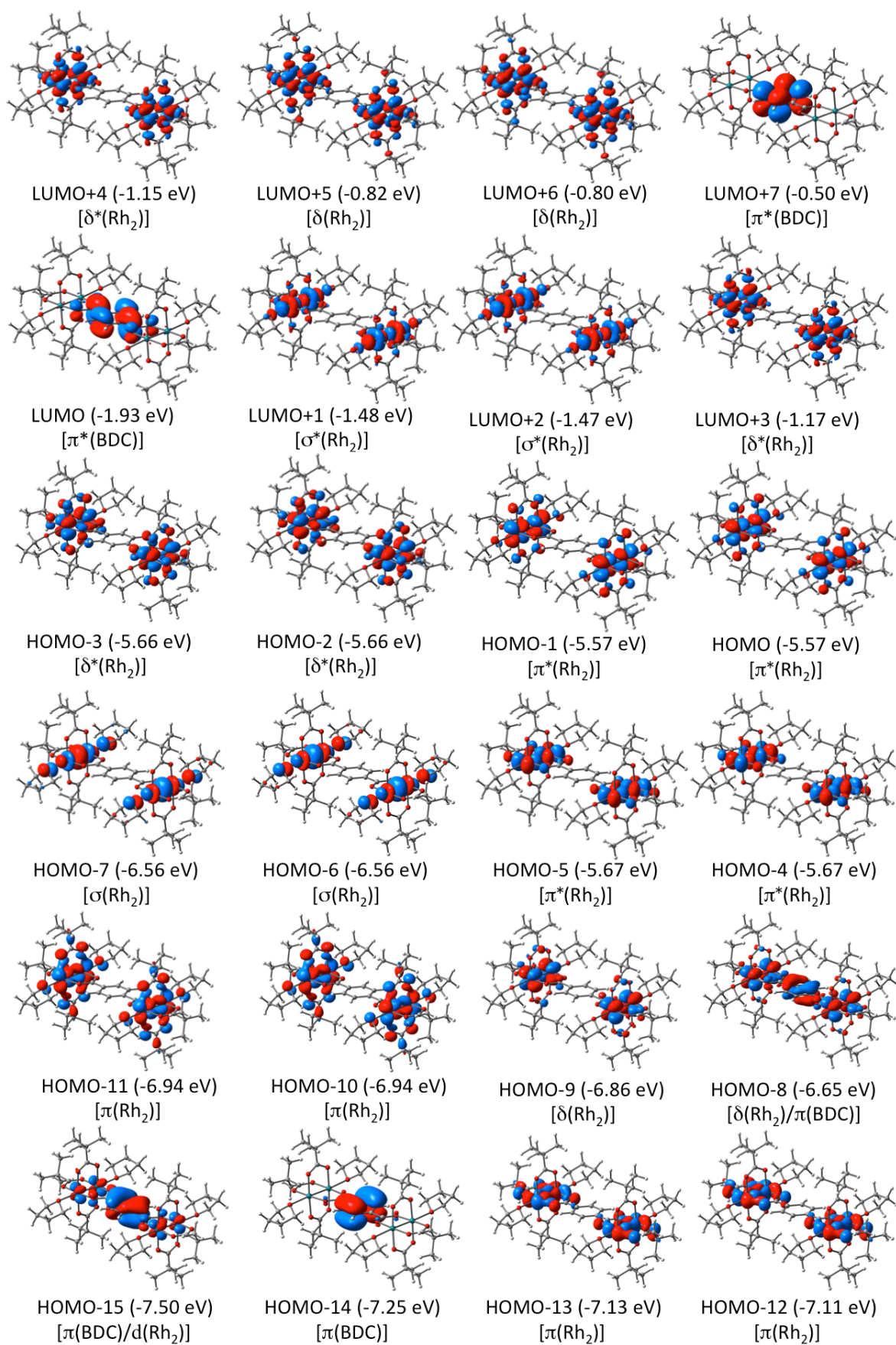


Figure S5. MOs of  $[1(\text{THF})_4]$ .

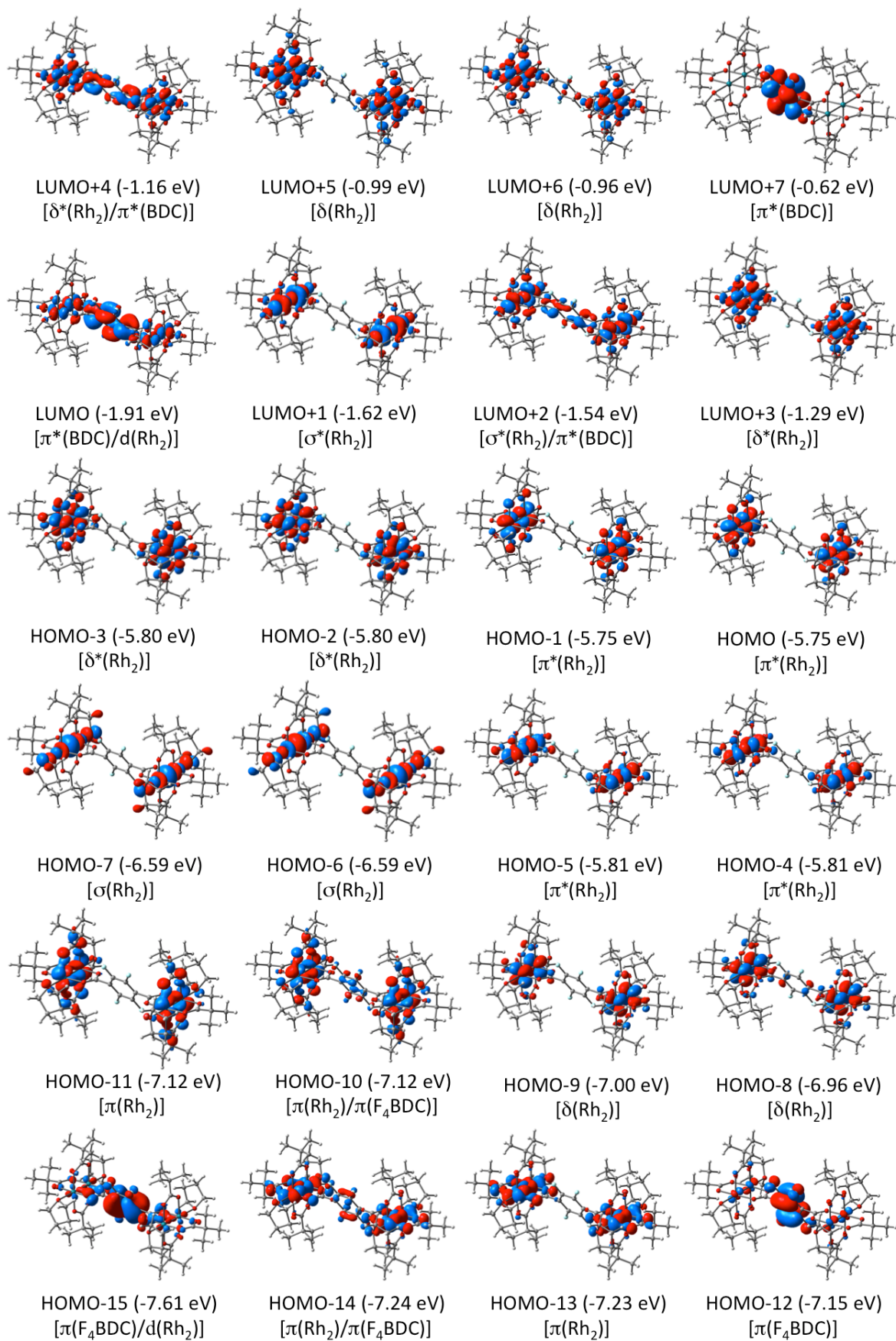


Figure S6. MOs of  $[2(\text{THF})_4]$ .

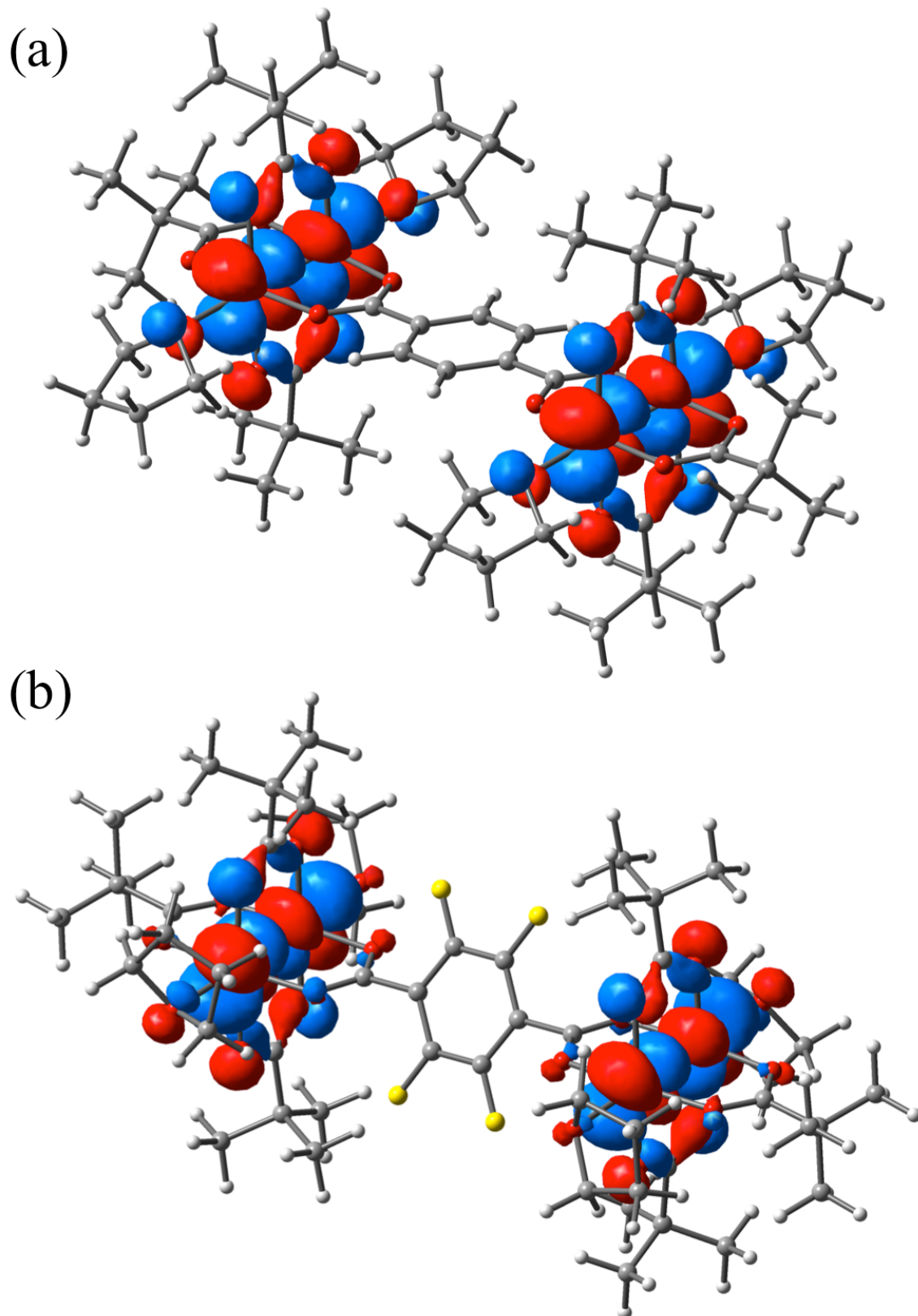


Figure S7. LUMOs ( $\beta$  orbitals) of  $[1(\text{THF})_4]^+$  and  $[2(\text{THF})_4]^+$ .

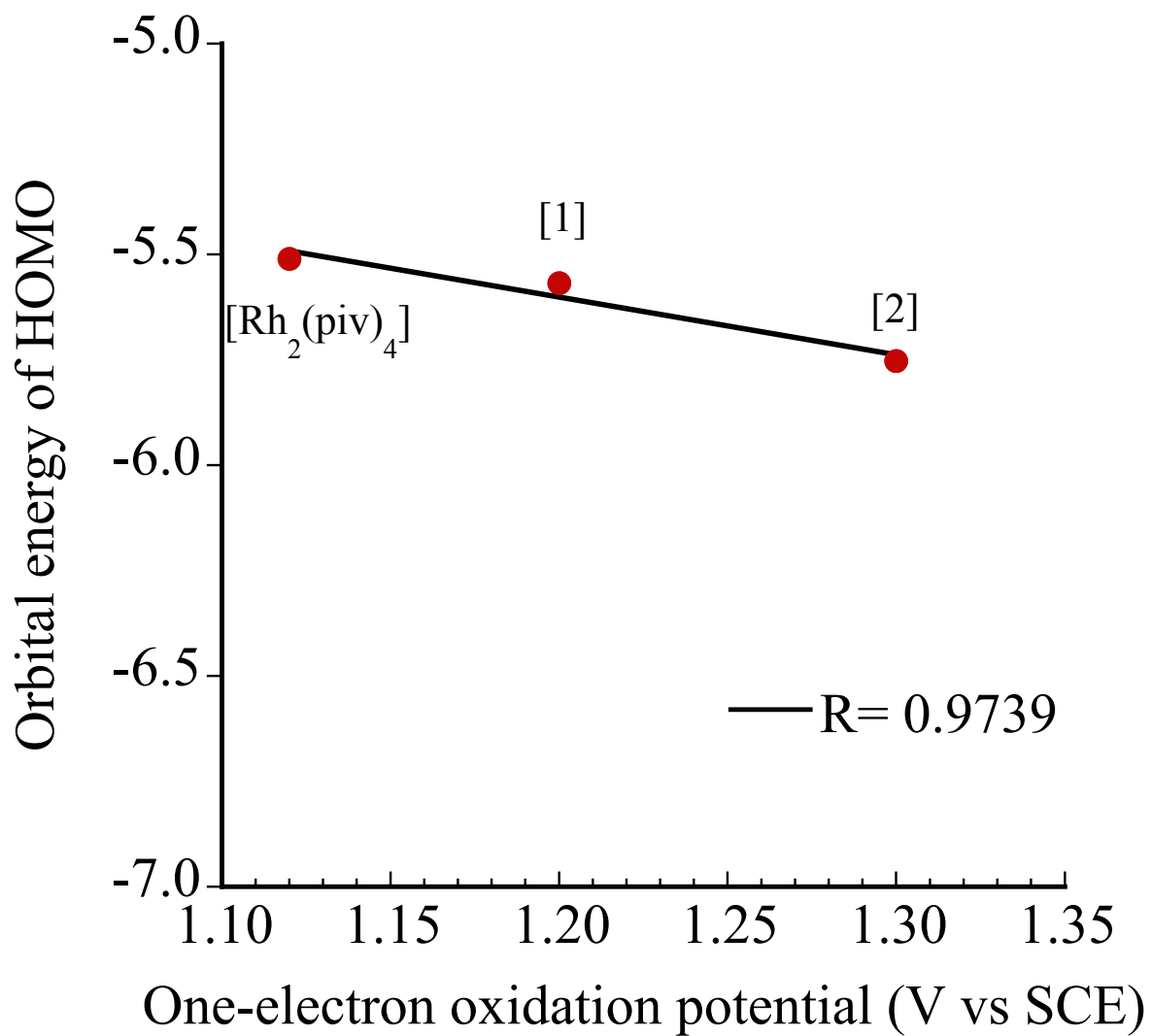


Figure S8. The plots of orbital energies of HOMOs vs. one-electron oxidation potentials of [1], [2], and [Rh<sub>2</sub>(piv)<sub>4</sub>].

Table S1. Selected structural parameters (bond lengths: Å, angles: °) of [1(THF)<sub>4</sub>].

Bond lengths (Å)			
Rh(1)-Rh(2)	2.3813(4)	O(1)-C(1)	1.259(4)
Rh(1)-O(1)	2.044(2)	O(2)-C(1)	1.264(4)
Rh(1)-O(3)	2.030(2)	O(3)-C(6)	1.261(4)
Rh(1)-O(5)	2.022(2)	O(4)-C(6)	1.264(4)
Rh(1)-O(7)	2.032(2)	O(5)-C(11)	1.274(4)
Rh(1)-O(9)	2.324(3)	O(6)-C(11)	1.265(4)
Rh(2)-O(2)	2.021(2)	O(7)-C(16)	1.263(4)
Rh(2)-O(4)	2.027(2)	O(8)-C(16)	1.267(4)
Rh(2)-O(6)	2.033(2)	C(16)-C(17)	1.487(5)
Rh(2)-O(8)	2.042(2)		
Rh(2)-O(10)	2.309(2)		
Bond angles (°)			
Rh(1)-Rh(2)-O(2)	88.65(7)	O(2)-Rh(2)-O(4)	89.88(11)
Rh(1)-Rh(2)-O(4)	88.11(7)	O(2)-Rh(2)-O(6)	176.35(10)
Rh(1)-Rh(2)-O(6)	87.95(7)	O(2)-Rh(2)-O(8)	88.37(11)
Rh(1)-Rh(2)-O(8)	88.24(7)	O(2)-Rh(2)-O(10)	89.65(10)
Rh(1)-Rh(2)-O(10)	177.53(6)	O(4)-Rh(2)-O(6)	88.67(11)
Rh(2)-Rh(1)-O(1)	87.52(7)	O(4)-Rh(2)-O(8)	175.99(9)
Rh(2)-Rh(1)-O(3)	88.11(7)	O(4)-Rh(2)-O(10)	90.09(10)
Rh(2)-Rh(1)-O(5)	88.42(7)	O(6)-Rh(2)-O(8)	92.85(10)
Rh(2)-Rh(1)-O(7)	88.18(7)	O(6)-Rh(2)-O(10)	93.71(10)
Rh(2)-Rh(1)-O(9)	176.34(7)	O(8)-Rh(2)-O(10)	93.51(9)
O(1)-Rh(1)-O(3)	89.83(11)	O(1)-C(1)-O(2)	125.8(3)
O(1)-Rh(1)-O(5)	175.80(9)	O(3)-C(6)-O(4)	125.8(3)
O(1)-Rh(1)-O(7)	88.89(11)	O(5)-C(11)-O(6)	125.1(3)
O(1)-Rh(1)-O(9)	96.14(10)	O(7)-C(16)-O(8)	126.2(3)
O(3)-Rh(1)-O(5)	88.95(12)	O(7)-C(16)-C(17)	117.2(3)
O(3)-Rh(1)-O(7)	176.12(10)	O(8)-C(16)-C(17)	116.6(3)
O(3)-Rh(1)-O(9)	91.78(10)	C(16)-C(17)-C(18)	120.5(3)
O(5)-Rh(1)-O(7)	92.07(11)	C(16)-C(17)-C(19)	121.5(3)
O(5)-Rh(1)-O(9)	87.92(10)	C(18)-C(17)-C(19)	118.0(3)
Dihedral angles (°)			
O(8)-C(16)-C(17)-C(19)	2.8(5)	O(7)-C(16)-C(17)-C(18)	3.4(5)

Table S2. Selected structural parameters (bond length: Å, angles: °) of [2(THF)<sub>4</sub>].

Bond lengths (Å)			
Rh(1)-Rh(2)	2.3865(4)	O(1)-C(1)	1.265(3)
Rh(1)-O(1)	2.0391(15)	O(2)-C(1)	1.269(3)
Rh(1)-O(3)	2.0285(15)	O(3)-C(6)	1.262(3)
Rh(1)-O(5)	2.0346(16)	O(4)-C(6)	1.268(3)
Rh(1)-O(7)	2.0582(15)	O(5)-C(11)	1.269(3)
Rh(1)-O(9)	2.3262(16)	O(6)-C(11)	1.265(3)
Rh(2)-O(2)	2.0223(16)	O(7)-C(16)	1.262(3)
Rh(2)-O(4)	2.0264(15)	O(8)-C(16)	1.254(3)
Rh(2)-O(6)	2.0396(15)	C(16)-C(17)	1.514(3)
Rh(2)-O(8)	2.0487(15)		
Rh(2)-O(10)	2.2884(17)		
Bond angles (°)			
Rh(1)-Rh(2)-O(2)	88.09(5)	O(2)-Rh(2)-O(4)	88.92(7)
Rh(1)-Rh(2)-O(4)	88.37(5)	O(2)-Rh(2)-O(6)	176.43(6)
Rh(1)-Rh(2)-O(6)	88.61(4)	O(2)-Rh(2)-O(8)	89.22(7)
Rh(1)-Rh(2)-O(8)	88.36(4)	O(2)-Rh(2)-O(10)	92.74(7)
Rh(1)-Rh(2)-O(10)	178.97(5)	O(4)-Rh(2)-O(6)	89.65(7)
Rh(2)-Rh(1)-O(1)	88.22(4)	O(4)-Rh(2)-O(8)	176.29(6)
Rh(2)-Rh(1)-O(3)	87.78(5)	O(4)-Rh(2)-O(10)	91.04(7)
Rh(2)-Rh(1)-O(5)	87.67(5)	O(6)-Rh(2)-O(8)	92.03(7)
Rh(2)-Rh(1)-O(7)	88.32(4)	O(6)-Rh(2)-O(10)	90.56(7)
Rh(2)-Rh(1)-O(9)	176.84(4)	O(8)-Rh(2)-O(10)	92.26(6)
O(1)-Rh(1)-O(3)	88.29(7)	O(1)-C(1)-O(2)	126.0(2)
O(1)-Rh(1)-O(5)	175.74(6)	O(3)-C(6)-O(4)	125.7(2)
O(1)-Rh(1)-O(7)	89.22(7)	O(5)-C(11)-O(6)	125.7(2)
O(1)-Rh(1)-O(9)	93.99(6)	O(7)-C(16)-O(8)	128.77(19)
O(3)-Rh(1)-O(5)	90.43(7)	O(7)-C(16)-C(17)	115.66(18)
O(3)-Rh(1)-O(7)	175.44(6)	O(8)-C(16)-C(17)	115.55(18)
O(3)-Rh(1)-O(9)	90.01(6)	C(16)-C(17)-C(18)	120.59(18)
O(5)-Rh(1)-O(7)	91.77(7)	C(16)-C(17)-C(19)	122.36(19)
O(5)-Rh(1)-O(9)	90.07(6)	C(18)-C(17)-C(19)	117.05(19)
Dihedral angles (°)			
O(8)-C(16)-C(17)-C(19)	78.3(3)	O(7)-C(16)-C(17)-C(18)	77.9(3)

Table S3. The averaged bond lengths ( $\text{\AA}$ ) of optimized geometries of **[1(THF)<sub>4</sub>]** and **[2(THF)<sub>4</sub>]**.

	<b>[1(THF)<sub>4</sub>]</b>	<b>[2(THF)<sub>4</sub>]</b>
Rh-Rh	2.413	2.418
Rh-O(BDC)	2.071	2.078
Rh-O(piv) ( <i>trans</i> -position vs. BDC)	2.066	2.055
Rh-O(piv) ( <i>cis</i> -position vs. BDC)	2.065	2.062
Rh-O(THF)	2.339	2.338

Table S4. TDDFT results (excitation energies, oscillator strengths, and assignments) of [1(THF)<sub>4</sub>].

State	Wavelength (nm)	Osc. Str. ( <i>f</i> )	Contribution
2	566.8	0.0090	H→L+2 (42%), H-1→L+1 (41%)
3	552.2	0.0081	H-4→L+1 (44%), H-5→L+2 (43%)
12	438.1	0.0033	H-1→L+3 (40%), H→L+4 (39%)
13	423.7	0.0051	H-4→L+3 (43%), H-5→L+4 (41%)
43	297.1	0.6768	H-8→L (96%)
49	289.4	0.0172	H-8→L+4 (37%), H-9→L+3 (31%)
53	278.4	0.0024	H-10→L (96%)
58	273.9	0.0026	H-8→L+6 (43%), H-9→L+5 (37%)
60	272.1	0.0029	H-13→L (95%)
67	269.9	0.0099	H-14→L (84%)
68	269.5	0.0025	H-4→L+5 (50%), H-5→L+6 (49%)
71	267.9	0.4668	H-7→L+1 (35%), H-6→L+2 (34%)
72	266.7	0.0158	H-2→L+7 (99%)
77	265.0	0.0032	H-12→L+3 (41%), H-13→L+4 (39%)
83	255.8	0.0022	H→L+11 (40%), H-1→L+8 (26%), H-1→L+12 (15%)
84	255.1	0.0013	H-4→L+8 (42%), H-5→L+9 (23%), H-5→L+11 (21%)
87	252.6	0.038	H-11→L+5 (42%), H-10→L+6 (40%)
89	252.4	0.0092	H-2→L+9 (41%), H-3→L+10 (34%), H-3→L+8 (11%)
94	247.8	0.2708	H-12→L+5 (39%), H-13→L+6 (37%), H-15→L (16%)
96	247.1	0.0211	H→L+14 (18%), H-3→L+8 (13%), H-1→L+8 (11%), H-1→L+12 (11%), H-1→L+15 (11%), H-2→L+11 (10%),
99	246.5	0.0523	H-3→L+8 (29%), H-2→L+11 (16%), H→L+14 (10%)
100	241.7	0.4474	H-15→L (76%)
101	241.1	0.0001	H-6→L+4 (50%), H-7→L+3 (49%)
112	235.6	0.0019	H-8→L+4 (49%), H-9→L+3 (43%)
116	234.2	0.1389	H-3→L+12 (23%), H-2→L+14 (19%), H-3→L+15 (12%)
118	232.3	0.0030	H-3→L+15 (22%), H-3→L+8 (20%), H-3→L+12 (16%), H-2→L+14 (12%)
120	231.6	0.0033	H-17→L (94%)

Table S5. TDDFT results (excitation energies, oscillator strengths, and assignments) of [2(THF)<sub>4</sub>].

State	Wavelength (nm)	Osc. Str. ( <i>f</i> )	Contribution
1	565.1	0.0093	H-5→L+1 (28%), H-4→L (18%), H-1→L+1 (12%)
4	554.2	0.0058	H-1→L+1 (29%), H→L+2 (28%), H-5→L+1 (13%), H-4→L+2 (10%)
12	444.7	0.0038	H→L (31%), H-1→L+3 (30%), H→L+4 (17%)
13	425.6	0.0051	H-5→L+3 (34%), H-4→L+2 (21%), H-4→L+4 (14%)
21	352.2	0.0014	H-2→L (32%), H-4→L (20%)
26	322.6	0.0053	H-7→L (39%), H-6→L+3 (32%), H-7→L+4 (16%)
27	319.9	0.0036	H-9→L+1 (39%), H-8→L+2 (23%), H-8→L (21%)
29	318.9	0.0018	H-11→L+1 (34%), H-10→L+2 (20%), H-10→L (14%)
33	314.3	0.0015	H-13→L+1 (36%), H-14→L+2 (20%), H-14→L (17%)
41	291.5	0.0202	H-9→L+3 (24%), H-8→L (18%), H-8→L+2 (14%), H-3→L+5 (12%), H-8→L+4 (11%)
44	289.6	0.0017	H-5→L+3 (33%), H-4→L+4 (29%), H-2→L+4 (18%)
45	289.4	0.0046	H-3→L+3 (31%), H-2→L+4 (27%), H-4→L+4 (20%), H-5→L+3 (11%)
50	284.7	0.0522	H-7→L (51%), H-6→L+3 (17%), H-7→L+4 (16%)
53	275.2	0.0014	H→L+6 (52%), H-1→L+5 (42%)
56	273.1	0.0647	H-9→L+5 (27%), H-8→L+6 (27%)
57	272.2	0.0030	H-2→L+6 (48%), H-3→L+5 (40%)
61	270.5	0.0083	H-13→L+3 (24%), H-14→L (21%), H-14→L+2 (16%),
64	270.0	0.3548	H-6→L+1 (43%), H-7→L+2 (18%)
65	268.5	0.0156	H-12→L (44%), H→L+7 (21%), H-4→L+7 (11%)
67	267.2	0.0053	H→L+7 (73%), H-12→L (13%)
69	264.9	0.0033	H-2→L+7 (87%)
71	264.0	0.0096	H-4→L+7 (76%), H-12→L (12%)
72	262.4	0.2568	H-8→L (46%), H-8→L+4 (20%), H-9→L+3 (13%)
74	261.1	0.0052	H-7→L+2 (55%), H-6→L+1 (34%)
77	260.2	0.0018	H-1→L+8 (49%), H-5→L+8 (21%)
79	258.4	0.0010	H-5→L+8 (46%), H-1→L+8 (25%)
83	255.7	0.0084	H-3→L+8 (68%), H-2→L+11 (12%)
84	252.4	0.0130	H-10→L (22%), H-10→L+4 (19%), H-11→L+3 (14%)

86	251.8	0.0298	H-11→L+5 (30%), H-10→L+6 (27%)
88	250.6	0.0043	H-5→L+9 (18%), H-4→L+10 (16%), H-14→L (14%)
90	249.3	0.0119	H-4→L+10 (17%), H-13→L+5 (12%), H-5→L+9 (13%)
93	248.4	0.0168	H-3→L+9 (36%), H-2→L+10 (32%)
94	247.6	0.0070	H-1→L+12 (15%), H-5→L+9 (14%), H-4→L+10 (10%)
96	247.0	0.0105	H-1→L+12 (20%), H-14→L+6 (12%), H-13→L+5 (12%), H→L+13 (12%)
99	246.4	0.0039	H-5→L+12 (34%), H-4→L+13 (17%), H-4→L+11 (15%)
103	244.0	0.0026	H-12→L+2 (78%)
104	243.1	0.1771	H-15→L (33%), H-8→L+2 (31%), H-9→L+1 (22%)
106	241.2	0.5371	H-15→L (56%), H-9→L+1 (20%), H-8→L+2 (16%)
108	239.5	0.0048	H-1→L+15 (40%), H→L+16 (30%), H→L+11 (10%)
110	238.3	0.1056	H-3→L+12 (31%), H-2→L+11 (19%)
114	234.8	0.0059	H-16→L (30%), H-19→L (21%), H-18→L+1 (18%), H-17→L+1 (10%),
118	233.2	0.0175	H-16→L (35%), H-19→L (20%), H-18→L+1 (16%)